PHILOSOPHICAL
TRANSACTIONS A

rsta.royalsocietypublishing.org

Research

The influence hydrogen atom addition has on charge switching during motion of the metal atom in endohedral $Ca@C_{60}H_4$ isomers

G. Raggi, E. Besley and A. J. Stace

Department of Physical and Theoretical Chemistry, School of Chemistry, University Park, Nottingham NG7 2RD, UK

Cite this article: Raggi G, Besley E, Stace AJ. 2016 The influence hydrogen atom addition has on charge switching during motion of the metal atom in endohedral $Ca@C_{60}H_4$ isomers. *Phil. Trans. R. Soc. A* **374**: 20150319.
http://dx.doi.org/10.1098/rsta.2015.0319

Accepted: 14 April 2016

One contribution of 12 to a theme issue 'Fullerenes: past, present and future, celebrating the 30th anniversary of Buckminster Fullerene'.

Subject Areas:
nanotechnology

Keywords:
fullerene, calcium, density functional theory, nanoswitch, endohedral

Author for correspondence:
A. J. Stace
e-mail: anthony.stace@nottingham.ac.uk

Density functional theory has been applied in a study of charge transfer between an endohedral calcium atom and the fullerene cage in $Ca@C_{60}H_4$ and $[Ca@C_{60}H_4]^+$ isomers. Previous calculations on $Ca@C_{60}$ have shown that the motion of calcium within a fullerene is accompanied by large changes in electron density on the carbon cage. Based on this observation, it has been proposed that a tethered endohedral fullerene might form the bases of a nanoswitch. Through the addition of hydrogen atoms to one hemisphere of the cage it is shown that, when compared with $Ca@C_{60}$, asymmetric and significantly reduced energy barriers can be generated with respect to motion of the calcium atom. It is proposed that hydrogen atom addition to a fullerene might offer a route for creating a bi-stable nanoswitch that can be fine-tuned through the selection of an appropriate isomer and number of atoms attached to the cage of an endohedral fullerene.

This article is part of the themed issue 'Fullerenes: past, present and future, celebrating the 30th anniversary of Buckminster Fullerene'.

1. Introduction

Metal-containing endohedral fullerenes can now be synthesized routinely and their chemical and physical properties characterized with considerable precision [1–3]. Recent density functional theory (DFT) calculations on the endohedral complex $Ca@C_{60}$ showed that movement of the calcium atom through the cavity of a

THE ROYAL SOCIETY
PUBLISHING

fullerene molecule resulted in changes to the distribution of charge across the surface of the doped cage [4]. It was shown that an energy path taken by a calcium atom moving through the centre of C_{60} has two identical, off-centre minima, and that the movement of both Ca and Ca^+ between these positions triggers a significant redistribution of charge on the surface of the fullerene [4]. Such behaviour, promoted by the motion of a metal atom between stable sites, could be viewed as forming the basis of a polarization nanoswitch [5,6]. However, the presence of equivalent off-centre minima and a negligible circumferential energy barrier, i.e. what is in effect a 'Mexican hat' potential, makes it difficult to confine the calcium atom to fixed locations. In the new calculations presented here, it is shown how energy minima and the location of a calcium atom in a fullerene can be perturbed by the addition of hydrogen atoms to the cage. This functionalization of a fullerene cage creates distinguishable sites that may form the foundation for a bi-stable molecular nanoswitch [5–7]. Such a concept could be realized by tethering the fullerene cage and thus restricting movement of the calcium atom to a single predefined path. Jorn *et al.* [8] achieved such a restriction by placing an endohedral fullerene containing a trapped lithium atom between two arrays of gold atoms which acted as electrodes. Tethered fullerenes have also been proposed as molecular transistors [9].

The new DFT calculations presented here are used to show in detail how energy minima and the extent of charge redistribution in $Ca@C_{60}$ and $Ca@C_{60}^+$ are affected by the addition of four hydrogen atoms to the cage in the form of $Ca@C_{60}H_4$ isomers. The results of preliminary calculations on $Ca@C_{60}H_6$ and $Ca@C_{60}H_{30}$ are also presented in order to demonstrate the extent to which the environment experienced by endohedral calcium can be modified. Despite the very high level of activity associated with the synthesis of endohedral fullerenes, there does not appear to be any experimental data on the exact structures discussed here. However, the individual components $C_{60}H_4$ [10–12] and $Ca@C_{60}$ have been synthesized (e.g. [13,14]).

Previous DFT calculations on fullerenes were successful in determining distribution of charge density on a C_{60} molecule in the presence of an electric field created by a point charge located outside the cage [15]. It has been shown that there is a very close correspondence between a DFT calculation of the polarization response of C_{60} to the presence of an external point charge and that obtained using a classical electrostatic theory [16] derived to treat dielectric materials. More recent DFT calculations have shown that when a charge is located inside C_{60} (or a carbon nanotube) the sign and magnitude of the polarization response depend very strongly on the precise position of the ion trapped inside the encapsulating cage [4]. It was proposed that this very evident distortion of the charge distribution on C_{60} in response to an applied electric field (charged atom) is a physical property that could be employed in the design of a molecular polarization switch. Building a device within a cage, such as a fullerene, that can act as a molecular switch would be a particularly good approach to maintaining geometric integrity.

2. Theory methods

The DFT calculations, as implemented in the Q-Chem quantum chemistry software package [17], have been undertaken at the B3LYP/6–31G* level of theory [18–21] on a series of $Ca@C_{60}H_4$ isomers. An earlier publication using the same approach reported the results of calculations on optimized structures of both neutral $Ca@C_{60}$ and charged $[Ca@C_{60}]^+$ endohedral fullerenes [4]. It was found that in the lowest energy configuration of the electronic ground state of neutral $Ca@C_{60}$, there was extensive charge redistribution between the metal atom and the carbon cage and that the calcium atom was located at a radial distance of $r = 1.22$ Å from the centre of C_{60} facing the centre of a hexagon. By contrast, the minimum energy ground state of $[Ca@C_{60}]^+$ has the calcium ion 1.21 Å away from the centre of C_{60} and facing the midpoint of an edge between two adjacent hexagons. The electronic ground state for $Ca@C_{60}$ was found to be a triplet [4], which is in agreement with previous results [13,14,22], and a doublet state was identified as the ground state of the $[Ca@C_{60}]^+$ cation. Properties of the latter have been investigated because there are electronic states of Ca^+ that are readily accessible using laser radiation and, therefore, photon control may offer a route to charge switching. Potential energy profiles for the calcium atom as it passes between minimum energy configurations are based on single-point calculations through the centre of the cage and partial atomic charges on the carbon and hydrogen atoms in the hydrogenated fullerenes have been calculated using a Mulliken population analysis [23].

3. Results and discussion

(a) Geometry and barriers to motion in Ca@$C_{60}H_4$ and $[Ca@C_{60}H_4]^+$

In total, there are 4190 possible isomers of $C_{60}H_4$; but only a very small number of these have been synthesized and their structures confirmed [10–12]. In addition to their chemistry, interest in the isomers of $C_{60}H_4$ has also examined the possibility that they may have superior hole-transport properties to those exhibited by the bare fullerene [24]. Improvements in hole transport have been linked to isomers that do not introduce significant perturbations to the delocalized highest occupied molecular orbital. Figure 1 shows six separate configurations of Ca@$C_{60}H_4$ that have been examined in these calculations, and these are based on moving single hydrogen atoms across one of the hemispheres. Only one of the $C_{60}H_4$ isomers chosen has been synthesized and the others have been selected to provide effective coverage of the hemisphere. Synthetic routes to $C_{60}H_4$ isomers appear to be very selective and preferentially populate adjoining 6–6 fused rings by 1,2 addition [10–12]. For each of the four carbon atoms involved in the addition of hydrogen, there is a transition from sp^2 to sp^3 hybridization, and for the fullerene cage as a whole, hydrogen atom addition does appear to bring about a re-ordering of molecular orbitals in some of the isomers chosen.

Earlier calculations showed that the energy minimum for Ca@C_{60} involved the calcium atom occupying a site located 1.22 Å from the geometric centre of the fullerene cage [4]. In terms of displacement of the atom from one side of the cage through the centre to an equivalent position on the opposite side, the calcium atom moved between two symmetric energy minima separated by a barrier of 1.48 eV. As already noted, the calcium atom would experience a 'Mexican hat' potential as it moved around the fullerene cage at a fixed distance of 1.22 Å from the geometric centre. With the introduction of hydrogen atoms, each of the isomers of Ca@$C_{60}H_4$ shown in figure 1 now has a distinct geometry and accompanying that change are new asymmetric energy barriers. With the calcium atom taking a path through the centre of the cage, figures 2 and 3 show the results of step-by-step calculations on the total energy of Ca@$C_{60}H_4$ and $[Ca@C_{60}H_4]^+$, respectively. For the configuration in figure 1*a*, the path taken was from $(-x, 0, 0)$ opposite a hydrogen atom directly to $(+x, 0, 0)$ passing through the geometric centre of the carbon atoms. For the remaining configurations (figure 1*b*–*f*), the axis was rotated such that $(-x, 0, 0)$ was located between two hydrogens from $(-x, 0, 0)$ to $(+x, 0, 0)$ passing through the centre; the $(0, 0, 0)$ position corresponds to the geometric centre of the fullerene cage. In all of the discussion that follows, it is the right hemisphere of the fullerene cage that accommodates the additional hydrogen atoms.

In comparison with the bare cage, the addition of hydrogen atoms to Ca@C_{60} introduces a number of changes to the magnitudes and positions of energy minima and maxima with respect to the movement of calcium across the fullerene cage. Most notable is the asymmetry in the energy profile, and in four out of the six neutral configurations examined, calcium favours a position adjacent to the hydrogen atoms; but for configurations of figure 1*d*,*f* there is a notable preference for a site in the opposite hemisphere. A similar asymmetry is seen in figure 3 for $[Ca@C_{60}H_4]^+$, but in this case all structures favour a site opposite the hydrogen atoms as being more stable than one in close proximity to the atoms. Quantitative data on the positions of the energy minima and heights of the energy barriers are summarized in tables 1 and 2, where for the purposes of comparison, the equivalent results for Ca@C_{60} and Ca@C_{60}^+ are also presented. For all configurations, calculations have been undertaken on electronic states with multiplicities of 1, 3 and 5 for the neutral species, and 2, 4 and 6 for the corresponding ionized species. For neutral Ca@C_{60} and ionic Ca@C_{60}^+, the electronic ground states were found to be triplet and doublet, respectively [4]. The results in table 1 show that the addition of hydrogen introduces

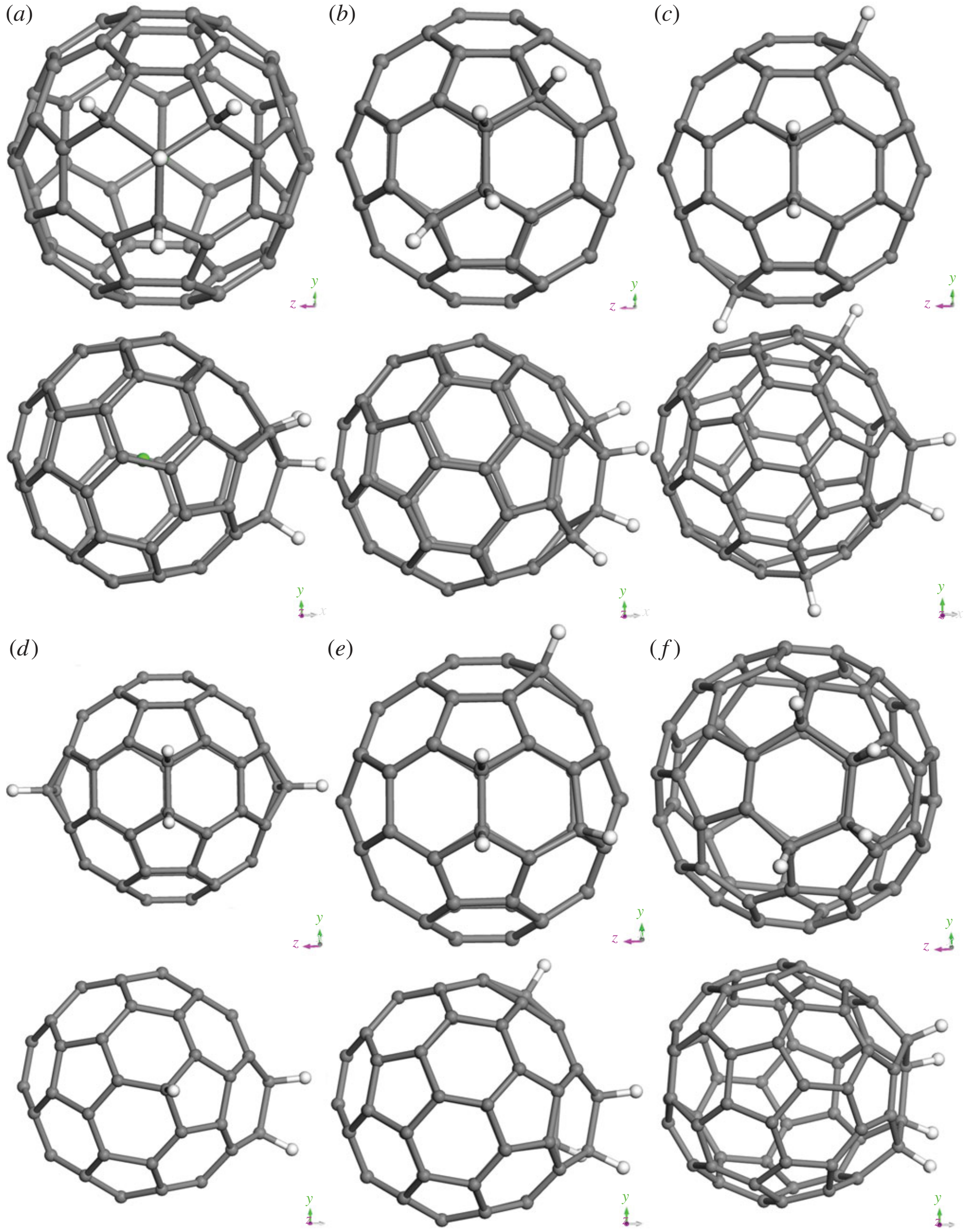

Figure 1. Six optimized configurations of neutral and ionized Ca@$C_{60}H_4$. Shown at the top of structures (*a*–*f*) is a 'front' view and underneath is a 'profile' view. Structure (*f*) is the only $C_{60}H_4$ combination known to have been synthesized. (Online version in colour.)

an interesting variation in the multiplicity of neutral Ca@$C_{60}H_4$ isomers. For configurations a–e, where hydrogen atoms have been allocated to a variety of sites involving both hexagons and pentagons, the multiplicity reverts to that of a singlet state. By contrast, configuration f has both the lowest total energy of all the permutations examined and also retains the triplet multiplicity of Ca@C_{60}. This observation would suggest that 1,2 hydrogen atom addition across adjoining 6–6 fused rings is not too disruptive to the underlying molecular orbital configuration of Ca@C_{60}. Isomer f is also the only isomer where calcium has been introduced into a known stable species [10–12].

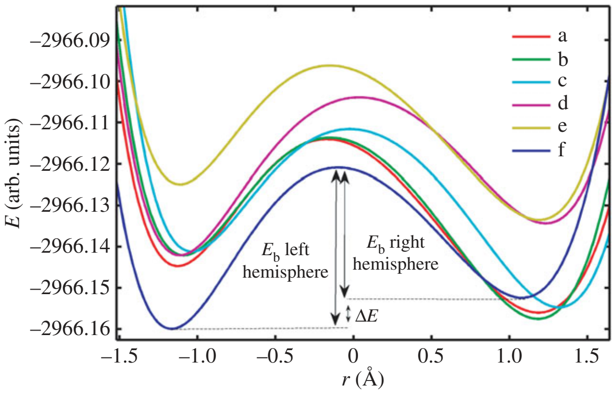

Figure 2. Total energy curves calculated for displacement along the *x*-axis of the calcium atom in neutral Ca@$C_{60}H_4$ in each of the six configurations shown in figure 1. The geometric centre of the fullerene cage is at $x = 0$ and the hydrogen atoms are located on the $+x$ side of the fullerene cage.

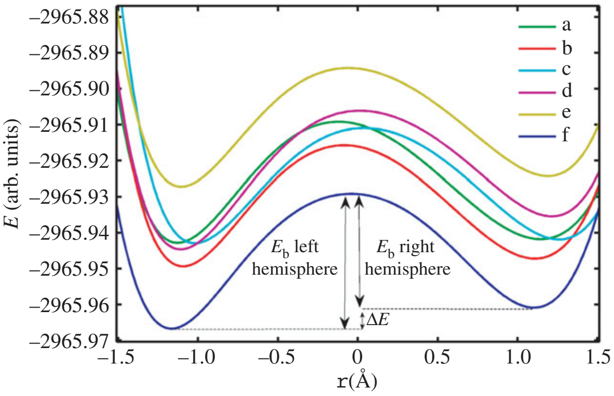

Figure 3. Same as figure 2, but for $[\mathrm{Ca@C_{60}H_4}]^+$.

Taking the results for Ca@C_{60} as a point of reference, it can be seen from table 1 that hydrogen atom addition brings about slight changes to the environment experienced by a calcium atom. There are shifts of approximately 0.1 Å in the locations of energy minima and maxima, but no systematic trends. Comparing Ca@$C_{60}H_4$ and $[\mathrm{Ca@C_{60}H_4}]^+$, there is little difference between the data given in tables 1 and 2, respectively. Common to both systems, when compared with Ca@C_{60} and Ca@C_{60}^+, is the significant reduction in magnitude of the energy barrier experienced by a calcium atom as it moves across each of the fullerene cages; in some instances, this reduction is almost a factor of two. ΔE values ($E_{\mathrm{bl}} - E_{\mathrm{br}}$, see figure 2) are, for the most part, lower in $[\mathrm{Ca@C_{60}H_4}]^+$ than those calculated for Ca@$C_{60}H_4$.

Since the calcium atom donates between one and two 4s electrons to the fullerene, an overall negative charge resides on the cage in Ca@C_{60}. However, depending on the position of the atom, a marked polarization of charge density has been observed and it was this pattern of behaviour that led to the proposal of a fullerene switch [4]. In order to help interpret the driving force(s) behind the changes that hydrogen atom addition brings about in Ca@$C_{60}H_4$ and $[\mathrm{Ca@C_{60}H_4}]^+$, a Mulliken population analysis has been undertaken of the distribution of partial atomic charge across the various atomic sites within each of the fullerenes shown in figure 1. A graphical illustration of the changes in charge that can take place on individual atoms as a calcium atom moves through the cage can be seen in figures 4 and 5. Each figure shows three separate snapshots derived from different atom positions within the configuration of figure 1*a* when in the form of Ca@$C_{60}H_4$ (figure 4) and $[\mathrm{Ca@C_{60}H_4}]^+$ (figure 5). In both cases, the different positions

Table 1. Energy barriers and positions of energy minima and maxima for the movement of calcium through neutral Ca@$C_{60}H_4$. Also shown are the equivalent data for Ca@C_{60}. The units of length are Å and the units of energy are eV.

			left hemisphere		max.	right hemisphere		
configuration	M[a]	rel. energy[b]	x[c]	E^{d}_{bl}	x[e]	x[c]	E^{d}_{br}	$\Delta E(E_{\mathrm{bl}} - E_{\mathrm{br}})$[f]
a	1	0.10	−1.1	0.88	−0.2	1.2	1.16	−0.28
b	1	0.06	−1.1	0.77	−0.2	1.2	1.19	−0.42
c	1	0.14	−1.0	0.79	−0.1	1.3	1.16	−0.37
d	1	0.47	−1.1	1.02	0	1.2	0.81	+0.21
e	1	0.71	−1.1	0.78	−0.2	1.1	1.01	−0.23
f	3	0	−1.2	1.03	−0.2	1.1	0.83	+0.20
Ca@C_{60}	3	—	−1.2	1.48	0.0	1.2	1.48	0.0

[a] Multiplicity.

[b] Relative total energies for each of the configurations shown in figure 1.

[c] Location of the energy minimum.

[d] Energy barrier for the displacement of calcium towards the geometric centre of $C_{60}H_4$.

[e] Location of the energy maximum for the movement of calcium through $C_{60}H_4$.

[f] Difference between energy minima in the left and right hemispheres of Ca@$C_{60}H_4$ (figure 2).

Table 2. Same as table 1, but for $[\mathrm{Ca@C_{60}H_4}]^{+}$. Also shown are the equivalent data for $[\mathrm{Ca@C_{60}}]^{+}$. All structures have doublet multiplicity.

		left hemisphere		max.	right hemisphere		
configuration	rel. energy[a]	x[b]	E^{c}_{b}	x[d]	x[b]	E^{c}_{b}	$\Delta E(E_{\mathrm{bl}} - E_{\mathrm{br}})$[e]
a	0.66	−1.1	0.90	−0.2	1.1	0.87	+0.03
b	0.47	−1.1	0.90	−0.1	1.1	0.84	+0.06
c	0.65	−1.0	0.86	0	1.3	0.82	+0.04
d	0.60	−1.1	1.03	0	1.2	0.77	+0.26
e	1.08	−1.1	0.89	−0.1	1.2	0.81	+0.08
f	0	−1.2	1.00	−0.1	1.1	0.83	+0.17
$[\mathrm{Ca@C_{60}}]^{+}$		−1.2	1.38	0.0	1.2	1.38	0.0

[a] Relative total energies for each of the configurations shown in figure 1.

[b] Location of the energy minimum.

[c] Energy barrier for the displacement of calcium towards the geometric centre of $C_{60}H_4$.

[d] Location of the energy maximum for the movement of calcium through $[\mathrm{C_{60}H_4}]^{+}$.

[e] Difference between energy minima in the left and right hemispheres of $[\mathrm{Ca@C_{60}H_4}]^{+}$.

correspond to the calcium atom moving along the x-axis ($y = 0$ and $z = 0$). In figure 4*a*, the atom is located −1.1 Å from the geometric centre of the cage, which corresponds to an energy minimum in the left hemisphere; figure 4*b* corresponds to the energy maximum seen at −0.2 Å and in figure 4*c* the calcium atom is located at the energy minimum in the right hemisphere, which occurs at +1.2 Å. The calcium atom donates electron density to the cage, which means that it carries a permanent positive charge over the entire path; however, charge density on the carbon atoms fluctuates from being negative (red circles) to positive (blue circles) according to their proximity to calcium. Apart from calcium, the only other atoms in Ca@$C_{60}H_4$ that remain

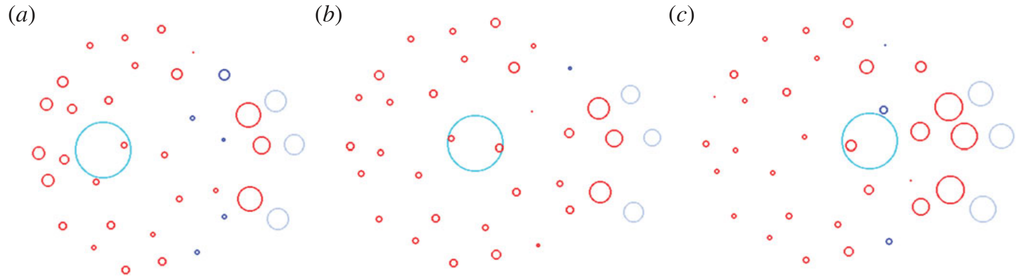

Figure 4. Distribution of partial atomic charge for three different positions of the calcium atom (blue cyan) in Ca@$C_{60}H_4$ (isomer a). The carbon atoms are depicted according to the charge they carry: red (negative) and blue (positive), and the hydrogens are the light blue circles. Rather than showing the magnitude of charge, the size of circle is renormalized according to the degree of polarization each atom experiences. Two of the hydrogen atoms overlap with one another.

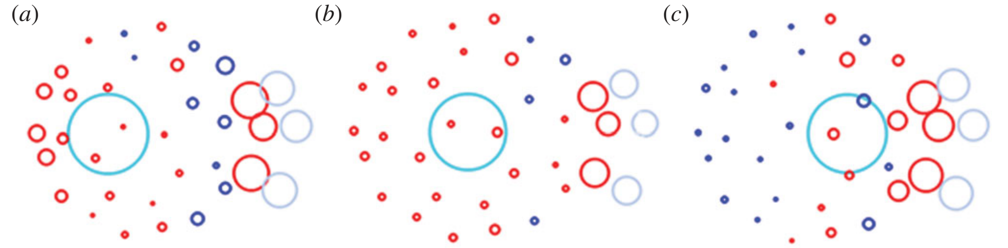

Figure 5. Same as figure 4, but taken from calculations on $[\mathrm{Ca@C_{60}H_4}]^+$.

permanently positive and insensitive to the exact location of the metal atom are the four hydrogen atoms which are depicted in figure 4 as light blue circles. Figure 5 shows the results of a similar analysis of Mulliken populations in $[\mathrm{Ca@C_{60}H_4}]^+$; however, because a single electron has now been removed from the complex, some of the carbon atoms in the cage retain a permanent positive charge irrespective of the position of the calcium atom. The consequences of this latter observation are seen below. Common to both figures 4 and 5 are a permanent positive charge on the hydrogen atoms and a permanent negative charge on the sp^3 carbon atoms.

An analysis of how motion of the calcium atom influences charge transfer and, as a result, the distribution of charge between the two hemispheres of Ca@$C_{60}H_4$ is shown in figure 6. Focusing on the left hemisphere, with the calcium atom at -1.1 Å (energy minimum), the charge averaged across the different isomers is approximately $-0.9e$. Moving to the energy maximum (-0.2 Å), the charge drops slightly to approximately $-0.86e$, and when the atom finally moves to an energy minimum in the right hemisphere (at $+1.2$ Å), the charge drops still further in magnitude to approximately $-0.3e$. These changes mean that the charge on the left hemisphere switches by approximately $0.6e$ as the calcium atom moves between the two energy minima. The presence of hydrogen atoms causes the carbon shell to become asymmetric during the optimization process; an effect due primarily to a change in hybridization where those carbon atoms that are bonded to hydrogen go from being sp^2 to sp^3. More significant, however, is the fact that sp^3 carbon atoms are much less electronegative than sp^2 hybrids. Interestingly, the charge maximum ($-1.03e$) in the left hemisphere does not coincide with the energy minimum, but is reached at -0.75 Å; however, for the right hemisphere there is a much closer correspondence between charge maximum and energy minimum. Figure 7 shows how charge on the fullerene cage responds to the formation of $[\mathrm{Ca@C_{60}H_4}]^+$. As for figure 6, the data are presented as a function of the position of the calcium atom on the x-axis. In contrast with the response from neutral Ca@$C_{60}H_4$, the data now show evidence of a very definite switch between negative and positive charge density; however, the

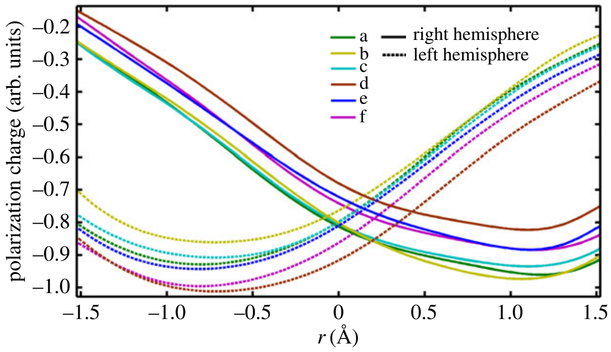

Figure 6. Charge (in units of *e*) located on separate hemispheres of the fullerene cage in neutral Ca@$C_{60}H_4$ as a function of the position of the calcium atom on the *x*-axis. Each of the six configurations in figure 1 is shown separately and results for the right hemisphere include contributions from the four hydrogen atoms.

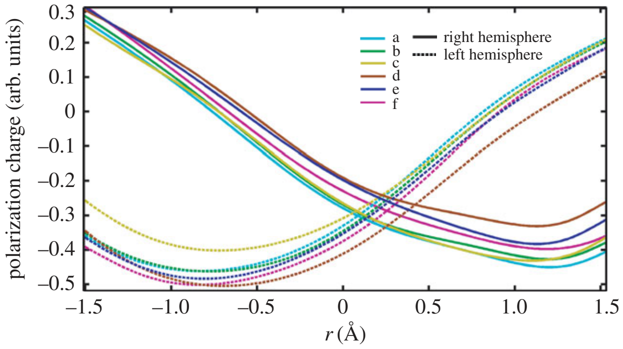

Figure 7. Same as figure 6, but for $[Ca@C_{60}H_4]^+$.

magnitude of the charge being displaced, approximately 0.6*e*, is still comparable with that seen for the neutral species. As noted for Ca@$C_{60}H_4$, there is again a mismatch in the left hemisphere between maximum charge displacement and the position of the energy minimum; however, this is not the case for the right hemisphere where the hydrogen atoms are located.

For each of the isomers, table 3 shows a more detailed breakdown of differences in the amount of charge residing on the two hemispheres as a function of the location of the calcium atom. Although the narrow spread in charge shown in figures 6 and 7 would suggest there is little difference between isomers, by tracking the changes that take place within individual examples a correlation between changes in charge and stability becomes apparent. As can be seen from table 3, the ability of the calcium atom to polarize charge in one or other of the hemispheres closely matches the changes in relative stability of the two extreme positions the atom can occupy. Overall, the differences in response from the two hemispheres to the motion of a calcium atom would appear to predominantly reflect the presence or absence of sp^3 carbon atoms, their positions on the cage and the influence they have on electronegativity. In all but two cases, an accumulation of excess charge in one or other of the two hemispheres appears to coincide with the calcium atom binding through an enhanced electrostatic interaction.

Finally, for the Ca@$C_{60}H_4$ series, figure 8 shows the change in electron density on the calcium atom as it moves through each of the isomers shown in figure 1. The plot summarizes data determined for both the neutral and ionic forms of Ca@$C_{60}H_4$. As expected from the results given above, the changes shown in figure 8 are more or less independent of which isomer is being examined; however, what is most surprising is that changes in charge are insensitive as to whether

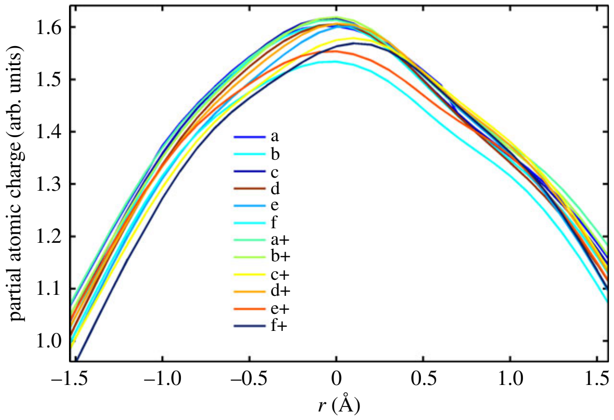

Figure 8. Charge (in units of *e*) calculated for calcium atoms in different positions within the fullerene cage, and for the six configurations of neutral and ionized Ca@$C_{60}H_4$ (ionized marked with a '+') given in figure 1.

Table 3. Absolute difference between the fraction of charge (figures 6 and 7) residing on the left and right hemispheres in selected isomers of Ca@$C_{60}H_4$ and $[Ca@C_{60}H_4]^+$ with the calcium atom in either of the minimum energy positions identified in figures 2 or 3.

		$\lvert\Delta Q\rvert$ (Ca)	
	isomer	left hemisphere	right hemisphere
Ca@$C_{60}H_4$	a	0.52	0.63[a]
	b	0.48	0.59[a]
	c	0.34	0.59[a]
	d	0.70[a]	0.35
	e	0.59	0.48[a]
	f	0.66[a]	0.45
$[Ca@C_{60}H_4]^+$	a	0.58[a]	0.55
	b	0.51[a]	0.52
	c	0.39[a]	0.56
	d	0.65[a]	0.35
	e	0.64[a]	0.47
	f	0.67[a]	0.46

[a] Configuration with the greater minimum energy.

or not Ca@$C_{60}H_4$ is either neutral or ionized. Given that the ionization energies of C_{60} and a calcium atom are 7.65 eV and 6.11 eV, respectively, it would be assumed that some fraction of 4s electron density on the atom would be lost as a consequence of forming $[Ca@C_{60}H_4]^+$; however, what appears to be the case is that ionization reduces electron donation from the atom to the cage by approximately 0.6*e*, but that the charge residing on the metal atom is largely unaffected by the process. For any given position of calcium within the cage, figure 8 shows the charge on the atom across all of the isomers to vary by just approximately 0.1*e*. These numbers are approximate and

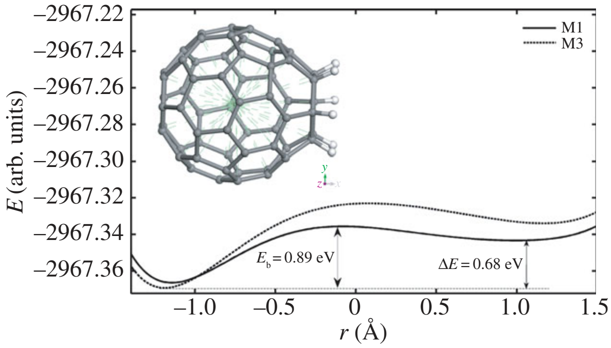

Figure 9. Total energy curves calculated for displacement along the *x*-axis of the calcium atom in neutral Ca@$C_{60}H_6$ for the configuration shown in the inset. The geometric centre of the fullerene cage is at $x = 0$ and the hydrogen atoms are located on the $+x$ side of the fullerene cage. (Online version in colour.)

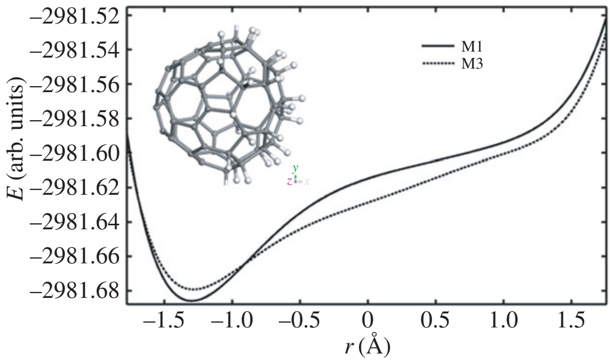

Figure 10. Same as figure 9, but for Ca@$C_{60}H_{30}$. (Online version in colour.)

reflect trends seen across the series of isomers under study; for an individual example, a detailed summation of charge on the cage and the calcium atom shows that ionization to the +1 state and the loss of an electron is balanced precisely by small changes in charge on each of the constituent atoms [4]. It has been found that the addition of 18 and 36 hydrogen atoms to the fullerene cage does reduce the ionization energy slightly, but the effect of just four atoms is most likely to be negligible [25].

(b) The effects of more extensive hydrogen atom addition

The results given above suggest that a change in hybridization from sp^2 to sp^3 in carbon atoms that form part of a fullerene cage could potentially create the conditions necessary for an endohedral fullerene of the form Ca@$C_{60}H_n$ to act as a polarization switch. Presented here are preliminary calculations on Ca@$C_{60}H_6$ and Ca@$C_{60}H_{30}$ that are intended to demonstrate the full extent to which hydrogen atom addition can modify the energy barrier to the motion of a metal atom in a fullerene cage. Figure 9 shows how the total energy of the fullerene Ca@$C_{60}H_6$ changes as a function of the location of the calcium atom. The exact structure chosen is shown in the inset. Similarly, figure 10 shows the consequences of completely decorating one-half of Ca@C_{60} with hydrogen atoms in the form of Ca@$C_{60}H_{30}$. As can be seen, in both structures there is some uncertainty as to the multiplicity of the ground state and it may require calculations of a greater accuracy to resolve this situation. However, what is clear for either multiplicity is that an increase in the number and/or density of sp^3 hybrid carbon atoms can lead to quite extensive modifications to the energy profile. With reference to the data in table 1, it can be seen that, while the barrier to exit from the left hemisphere is largely unaffected by the presence of the hydrogen atoms, there is a sharp drop in barrier height for movement out of the right hemisphere with the addition of just two further H atoms. On moving to $Ca@C_{60}H_{30}$, figure 10 shows that it is possible to remove completely an attractive interaction between the calcium atom and that half of the fullerene cage that is completely decorated with hydrogen atoms. For the most part, these effects appear to be driven by the marked drop in electron affinity shown by sp^3 carbon atoms, thus reducing the degree of electron donation from the calcium atom, which in turn diminishes the attractive electrostatic interaction that is responsible for creating the barriers.

4. Conclusion

Through DFT calculations, it has been shown that hydrogen atom addition to a fullerene cage offers the potential for fine-tuning the electronic and mechanical properties of endohedral $Ca@C_{60}H_4$ complexes. It is shown that changes in electronegativity that accompany a transition in hybridization for carbon from sp^2 to sp^3 influence the interaction between the calcium atom and the fullerene cage. However, compared with $Ca@C_{60}$, hydrogen atom addition does not appear to have a significant effect on the changes in charge polarization that occur as a result of the calcium atom moving through the fullerene. The changes in binding energy that accompany the formation of $Ca@C_{60}H_4$ remove the 'Mexican hat' potential observed previously for $Ca@C_{60}$ and create an asymmetric energy surface; therefore, it is proposed that certain isomers of $Ca@C_{60}H_4$ may form the bases of a bi-stable nanoswitch. Such a process may be facilitated by the fact that combinations of the individual components, i.e. $Ca@C_{60}$ and $C_{60}H_4$, have already been synthesized.

Competing interests. We declare we have no competing interests.

Funding. E.B. acknowledges an ERC Consolidator Grant for financial support. G.R. acknowledges the CONACYT Mexico Scholarship for PhD funding (Reg. 215343).

Acknowledgements. Both E.B. and A.J.S. worked at the University of Sussex during the time when Harry Kroto was actively engaged in fullerene chemistry. For over 20 years, A.J.S. was a staff member in chemistry at the university and experienced the entire evolution of fullerene science, from the observation of a pair of peaks in a mass spectrum in 1984/85, through the synthesis of solid samples in 1990 and finally to the award of a Nobel Prize in 1996. Harry was a very creative research scientist who was also prepared to invest time inspiring audiences of all descriptions with his passion for science—we welcome the opportunity we had to work with him.

References

1. Shinohara H. 2000 Endohedral metallofullerenes. *Rep. Prog. Phys.* **63**, 843–892. (doi:10.1088/0034-4885/63/6/201)
2. Popov AA, Yang S, Dunsch L. 2013 Endohedral fullerenes. *Chem. Rev.* **113**, 5989–6113. (doi:10.1021/cr300297r)
3. Lebedeva MA, Chamberlain TW, Khlobystov AN. 2015 Harnessing the synergistic and complementary properties of fullerene and transition-metal compounds for nanomaterial applications. *Chem. Rev.* **115**, 11 301–11 351. (doi:10.1021/acs.chemrev.5b00005)
4. Raggi G, Stace AJ, Bichoutskaia E. 2014 Polarisation charge switching through the motion of metal atoms trapped in fullerene cages. *Phys. Chem. Chem. Phys.* **16**, 23 869–23 873. (doi:10.1039/C4CP02672A)
5. Raehm L, Sauvage J-P. 2001 Molecular machines and motors based on transition metal-containing catenanes and rotaxanes. In *Molecular machines and motors* (eds J-P Sauvage *et al.*). Structure and Bonding, vol. 99, pp. 55–78. Berlin, Germany: Springer. (doi:10.1007/3-540-44421-1_3)
6. Kay ER, Leigh DA, Zerbetto F. 2007 Synthetic molecular motors and mechanical machines. *Angew. Chem. Int. Ed.* **46**, 72–191. (doi:10.1002/anie.200504313)
7. Pathem BK, Claridge SA, Zheng YB, Weiss PS. 2013 Molecular switches and motors on surfaces. *Annu. Rev. Phys. Chem.* **64**, 605–630. (doi:10.1146/annurev-physchem-040412-110045)

8. Jorn R, Zhao J, Petek H, Seideman T. 2011 Current-driven dynamics in molecular junctions: endohedral fullerenes. *ACS Nano* **5**, 7858–7865. (doi:10.1021/nn202589p)
9. Stokbro K. 2010 First-principles modelling of molecular transistors. *J. Phys. Chem. C* **114**, 20 461–20 465. (doi:10.1021/jp104811r)
10. Henderson CC, Rohlfing CM, Assink RA, Cahill PA. 1994 $C_{60}H_4$: kinetics and theromodynamics of multiple addition to C_{60}. *Angew. Chem. Int. Ed. Engl.* **33**, 786–788. (doi:10.1002/anie.199407861)
11. Avent AG *et al*. 1994 Formation of hydrids of fullerene-C_{60} and fullerene-C_{70}. *J. Chem. Soc. Perkin Trans.* **2**, 15–22. (doi:10.1039/p29940000015)
12. Cahill PA, Rohlfing CM. 1996 Theoretical studies of derivatised buckyballs and buckytubes. *Tetrahedron* **52**, 5247–5256. (doi:10.1016/0040-4020(96)00128-7)
13. Wang LS, Alford JM, Chai Y, Diener M, Zhang J, McClure SM, Guo T, Scuseria GE, Smalley RE. 1993 The electronic structure of Ca@C_{60}. *Chem. Phys. Lett.* **207**, 354–359. (doi:10.1016/0009-2614(93)89013-8)
14. Wang LS, Alford JM, Chai Y, Diener M, Smalley RE. 1993 Photoelectron spectroscopy and electronic structure of Ca@C_{60}. *Z. Phys. D* **26**, 297–299. (doi:10.1007/BF01425696)
15. Raggi G, Stace AJ, Bichoutskaia E. 2013 Surface-charge distribution on a dielectric sphere due to an external point charge: examples of C_{60} and C_{240}. *Phys. Chem. Chem. Phys.* **15**, 20 115–20 119. (doi:10.1039/c3cp53522c)
16. Bichoutskaia E, Boatwright AL, Khachatourian A, Stace AJ. 2010 Electrostatic analysis of the interactions between charged particles of dielectric materials. *J. Chem. Phys.* **133**, 024105. (doi:10.1063/1.3457157)
17. Shao Y *et al*. 2006 Advances in methods and algorithms in a modern quantum mechanical program package. *Phys. Chem. Chem. Phys.* **8**, 3172–3191. (doi:10.1039/B517914A)
18. Becke AD. 1993 Density-functional thermochemistry 3. The role of exact exchange. *J. Chem. Phys.* **98**, 5648–5652. (doi:10.1063/1.464913)
19. Lee C, Yang W, Parr RG. 1988 Development of the Colle-Salvetti correlation-energy formula into a functional of the electron density. *Phys. Rev. B* **37**, 785–789. (doi:10.1103/PhysRevB.37.785)
20. Hehre WJ, Ditchfier R, Pople J. 1972 A self-consistent molecular-orbital methods XII. Further extensions of Gaussian-type basis sets for use in molecular-orbital studies of organic molecules. *J. Chem. Phys.* **56**, 2257–2261. (doi:10.1063/1.1677527)
21. Rassolov VA, Ratner MA, Pople JA, Redfern PC, Curtiss LA. 2001 6-13G∗ basis set for third-row elements. *J. Comput. Chem.* **22**, 976–984. (doi:10.1002/jcc.1058)
22. Lu J, Zhang XW, Zhao XG. 1999 Electronic structures of endohedral Ca@C_{60}, Sc@C_{60} and Y@C_{60}. *Solid State Commun.* **110**, 565–568. (doi:10.1016/S0038-1098(99)00098-8)
23. Mulliken RS. 1955 Electronic population analysis on LCAO-MO molecular wave functions. *J. Chem. Phys.* **23**, 1833–1840. (doi:10.1063/1.1740588)
24. Tokunaga K, Kawabata H, Matsushige K. 2008 Improvement in hole-transport property of fullerene materials by hydrogenation: a density functional theory study of the fullerene hydride $C_{60}H_4$. *Jpn J. App. Phys.* **47**, 3638–3642. (doi:10.1143/JJAP.47.3638)
25. Populay AV, Abzalimov RR, Nasibullaev SK, Lobach AS, Drewello T, Vasil'ev YV. 2004 Ionization energies of the C_{60} fullerene and its hydrogenated derivatives $C_{60}H_{18}$ and $C_{60}H_{36}$ determined by electron ionization. *Int. J. Mass Spectrom.* **233**, 165–172. (doi:10.1016/j.ijms.2003.12.016)